Bachelor Thesis:

Design and setup of an intensity and polarization stabilization system for diode lasers

Robin Wanke

23.08.2012

5. Physikalisches Institut
University of Stuttgart, Germany

Prof. Dr. Tilman Pfau
Dr. Sebastian Hofferberth
5th Institute of Physics
University of Stuttgart

Declaration

I hereby declare that I have written this thesis on my own and I only used the utilities and resources which I have listed.

Stuttgart, 22.8.2012, Robin Wanke

German introduction

Diese Arbeit beschäftigt sich mit der Intensitäts- und Polarisationsstabilisierung eines Laserstrahls.
Laser finden sich in der experimentellen Physik in nahezu allen Laboren. Es kann sehr praktisch sein, dass Laser vom Experiment getrennt sind und deshalb kommt es häufig dazu, dass ein Laserstrahl von einem optischen Tisch auf einen anderen geführt werden muss. Dies kann zum Beispiel durch Benutzen einer optischen Faser geschehen. Um einen Laserstrahl in eine Faser koppeln zu können wird dieser auf eine Größe von meistens 5 µm fokussiert (für single mode fasern bei 780 nm). Das hat zur Folge, dass jede kleine mechanische Erschütterung die Kopplung verädert. Das führt zu einer Intensitätsschwankung am anderen Ende der Faser. Eine solche Faser ist meistens polarisationserhaltend. Wird nach der Faser ein Polarisationsstrahlteiler angebracht, kann über die Intensitätsstabilisierung auch automatisch die Polarisation stabilisiert werden.
Ein weiterer wichtiger Bestandteil dieser Arbeit ist ein akustooptischer Modulator. Dieser kann durch Schallwellen den Laserstrahl ablenken und so durch Variation der Schallwellenintensität die Laserintensität modulieren. Dieser Effekt wird ausgenutzt indem der akustooptische Modulator in einen Regelkreis eingebracht wird, der des Weiteren noch aus einem PID-Regler besteht. Der PID-Regler hat viele Verwendungsgebiete, für die Bachelor Arbeit wird ein PID-Regler nach Vorbild eines für die Frequenzstabilisierierung verwendeten PID-Reglers gebaut und entsprechend für die Intensitätsstabilisierung konfiguriert.
In dieser Arbeit ist es außerdem sehr wichtig die Grundzüge der Regelungstechnik kennen zu lernen. So wird zu Anfang dieser Arbeit der akustooptische Modulator analysiert und seine Charakteristika gemessen. Dasselbe wird auch für den PID-Regler durchgeführt. Am Schluss wird der ganze Regelungskreis vermessen und die Stabilität bestimmt.

Contents

1 Motivation

This thesis is about stabilizing the intensity and the polarization of a laser beam.
Lasers are used in many laboratories in experimental physics. It can be handy to separate the Laser source from the actual experiment. So it is quite common that optical fibers are used to transfer a laser beam from one place to another. This happens by coupling the laser beam into an optical fiber with an input diameter of about 5 μm (for single mode fibers for 780 nm), which makes the system very sensitive to any mechanical motion. A result of that is that the laser intensity drifts after the optical fiber. Optical fibers can also be polarization maintaining, so if a polarization beam splitter is used after the optical fiber, not only can the intensity be stabilized but also the polarization.
A device that can modulate a laser beam's intensity is an acoustooptical modulator. A sound wave is sent through the acoustooptical modulator, which causes a refraction of the laser beam. The intensity of the refraction can be changed by changing the intensity of the sound wave. The acoustooptical modulator is used for this thesis within the control circuit.
Another device of the control circuit is a PID controller that can be used for many purposes. The PID controller for this thesis is built by configuring a PID controller that is used for stabilization of a laser frequency. The PID controller is used to compensate as much intensity fluctuation as possible.
Another very important aspect of this bachelor thesis is to get to know how important electronics and control theory are for an experimental physicist.

Thesis outline

This thesis is structured into three main parts: The acoustooptical modulator, the PID-controller and the complete control circuit.
At first the thesis will give a short introduction to the theory of an acoustooptical modulator. Subsequently the acoustooptical modulator will be experimentally analyzed and characterized.
The second section starts with a very brief introduction to control theory and its application on a PID-controller. After this, the PID-controller that was built during this thesis will be analyzed and characterized.
The stability of the complete control circuit will be characterized in the last section.

2 The acoustooptical modulator

2.1 Theory

The acoustooptical modulator (AOM) is a very common optical device. It allows modulating the power of a laser beam or even switching the beam off and on without having to change the laser source. The basic idea of an AOM is the interaction between sound and light, more precisely, the effect of sound on the refraction index of an optical medium, which than modifies the propagation of light.

When sound passes through an optical medium, the molecules vibrate. Those vibrations cause a change of density in the medium, through compression and rarefaction. In areas of compression the refraction index is larger, whereas in areas of rarefaction the refractive index is smaller. Therefore sound is described as a wave of density running through a medium at the velocity of sound.

The perturbation of the refraction index is slow enough, that it can be considered as frozen, when looking at the time scale of light. Consequently, the medium can be approximated as a static medium with a periodically varying refractive index (figure 1). The periodicity can be controlled by varying the wavelength of sound.

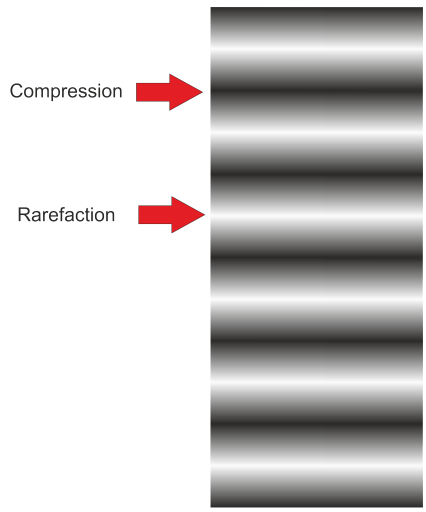

Figure 1: A sound wave running through a medium

Density perturbation

Since the refraction index is changing when an acoustic wave passes a medium, we are interested in how big the changes of the refraction index (Δn) are. We consider a plane wave that travels in the x-direction. We use

$$S(x,t) = S_0 \cos(\Omega t - k_{\mathrm{S}} x) \tag{2.1}$$

to describe the strain caused by the sound wave. Where S_0 is the amplitude, Ω is the angular frequency and $k_{\rm S}$ is the wavenumber.
The refraction index n is dependent on $S(x,t)$. Since we expect Δn to be small we can expand $n(S)$ in a Taylor's series about $S(x,t) = 0$:

$$n(S) = n - a_1 \cdot S \ ... \tag{2.2}$$

With $a_1 = \frac{\mathrm{d}n(S)}{\mathrm{d}S}$ at $S(x,t) = 0$. The refraction index can be written, using the photo elastic constant $\beta = -\frac{2a_1}{n^3}$ [1] as

$$n(x,t) = n - \frac{1}{2}\beta n^3 S(x,t). \tag{2.3}$$

$\Delta n_0 = \frac{1}{2}\beta S_0$ can be identified as the amplitude of the perturbation.
The intensity of an acoustic wave is the product of the sound pressure and its velocity. So with equation 2.1 the intensity can be written as [1]

$$I_{\rm S} = \frac{1}{2}\rho v_{\rm S}^3 S_0^2, \tag{2.4}$$

where ρ is the mass density of the medium and $v_{\rm S}$ the velocity of sound in the medium. Using equation 2.4 Δn_0 can be expressed with a parameter ζ which only dependents on material constants.

$$\Delta n_0 = \sqrt{\frac{1}{2}\zeta I_{\rm S}} \qquad \text{with} \qquad \zeta = \frac{\beta^2 n^6}{\rho v_{\rm S}^3} \tag{2.5}$$

Quantum mechanic view on acousto optics

Sound waves can be seen as waves on the one hand and on the other hand as particles (phonons). Let's look at an incoming photon with an energy of $\hbar\omega$ and a momentum $\hbar\vec{k}$ and a phonon with an energy of $\hbar\Omega$ and a momentum $\hbar\vec{q}$. Both particles can combine to a new photon, considering the conservation of energy and of the momentum, the new photon has a different energy $\hbar\omega + \hbar\Omega = \hbar\omega_r$ and a different momentum $\hbar\vec{k} + \hbar\vec{q} = \hbar\vec{k}_r$.
It is also possible that one incoming photon combines with two or more phonons to a new photon. So the energy and the momentum of the emerged photons can be

$$\hbar\omega_r = \hbar\omega + n \cdot \hbar\Omega \tag{2.6}$$

$$\hbar\vec{k}_r = \hbar\vec{k} \pm n \cdot \vec{q} \qquad\qquad n \in \mathbb{N}. \tag{2.7}$$

AOM-Types

There are two common types of AOMs, the Bragg-Type modulator and the Raman-Nath-Type Modulator.

Raman-Nath-Type modulator

An incoming light beam is perpendicular to the sound beam in the Raman-Nath-Type modulator. The sound beam is kept thin, so for the light beam it seems that the sound beam forms like a two dimensional diffraction grating. Therefore light is diffracted into many diffraction orders. The output beams emerge at an angle of $\theta \approx \frac{\lambda}{\Lambda}$ [1] with respect to the next diffraction orders. The intensity of the different orders can be expressed by an ordinary Bessel function [6]

Bragg-Type Modulator

This is the type of modulator that is used for this bachelor thesis. We will now look at the periodic structure of a planar sound wave and its effect on light reflection. Each layer transmits and reflects light, so in order to have constructive interference the path difference has to be an integer multiple of the wavelength. This is only possible if the incoming light beam has a precise

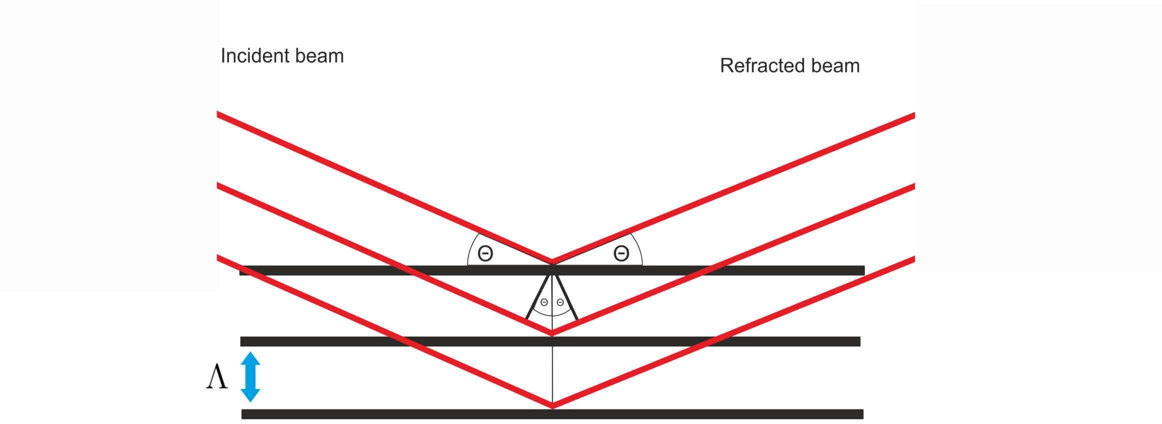

Figure 2: Reflection of a laser beam from different layers in the inhomogeneous medium

angle (compare figure 2). So the condition for constructive interference is

$$\sin(\Theta_{\mathrm{B}}) = \frac{n \cdot \lambda}{2\Lambda} \qquad n \in \mathbb{N}, \tag{2.8}$$

where Λ is the wavelength of the sound wave and λ the wavelength of the light beam. This is called the Bragg-Law or the Bragg-Condition. The diffracted output beam emerges at an angle of $2\theta_{\mathrm{B}}$ with respect to the no diffracted beam.

The Bragg type modulator has a higher efficiency than the Raman-Nath type modulator. By using the Bragg angle, the Bragg reflection could have an efficiency up to 100 %. But in practice, the efficiency can reach only up to around 90 %, when using an optimized beam waist, which will be discussed in detail in the experimental part.

Coupled wave theory

Let us look at the refraction process from a different point of view. Light going through an inhomogeneous medium that has a dynamic refraction index can also be described by a scattering

process.
The propagation of light in a normal homogeneous medium can be described by the wave equation [1]

$$\nabla^2 \vec{E} - \frac{1}{c_0^2}\frac{\partial^2 \vec{E}}{\partial t^2} = \mu_0 \frac{\partial^2 \vec{P}}{\partial t^2}, \tag{2.9}$$

here μ_0 is the magnetic permeability, $\vec{E}$ the electric field, c_0 the speed of light in vacuum and $\vec{P}$ the electric polarization density. In order to determine an equation for a nonlinear medium we have to look at $\vec{P}$. $\vec{P}$ can be written as a sum of linear and nonlinear parts, $\vec{P} = \epsilon_0 \chi \vec{E} + \vec{P}_{\text{nl}}$. Where ϵ_0 is the permittivity of free space and χ the electric susceptibility. The refraction index can be described by $n = \frac{1}{\sqrt{\epsilon_0 \mu_0}}$ and $n^2 - 1 = \chi$. The speed of light in a medium is given by $c = \frac{c_0}{n}$. Using all this relations, equation 2.9 can be rewritten as

$$\nabla^2 \vec{E} - \frac{1}{c_0^2}\frac{\partial^2 \vec{E}}{\partial t^2} = \mu_0 \epsilon_0 \chi \frac{1}{c_0^2}\frac{\partial^2 \vec{E}}{\partial t^2} + \mu_0 \frac{\partial^2 \vec{P}_{\text{nl}}}{\partial t^2} \tag{2.10}$$

$$\Rightarrow \nabla^2 \vec{E} - \frac{1}{c^2}\frac{\partial^2 \vec{E}}{\partial t^2} = -\vec{S} = \mu_0 \frac{\partial^2 \vec{P}_{\text{nl}}}{\partial t^2}. \tag{2.11}$$

Equation 2.11 is called the nonlinear wave equation, with $\vec{S}$ being a source of light.
Due to a perturbation of the refraction index we assume that a perturbation of the electric polarization density $\Delta\vec{P}$ can be seen as a source of light. So $\vec{P}_{\text{nl}} = \Delta\vec{P}$. We will look for an expression for $\Delta\vec{P}$. As used above $\vec{P} = \epsilon_0 \chi \vec{E} = \epsilon_0(n^2 - 1)\vec{E}$. n is not a constant if a sound wave goes through the medium, it is $n + \Delta n$. Now $\vec{P}$ becomes $\vec{P} = \epsilon_0(n^2 + 2n\Delta n)\vec{E}$. We can see that the perturbation of the electric polarization density is $\Delta\vec{P} = 2\epsilon_0 n(\Delta n \vec{E})$. So equation 2.11 changes to

$$\vec{S} = -2\mu_0 \epsilon_0 n \frac{\partial^2}{\partial t^2}(\Delta n \vec{E}). \tag{2.12}$$

There are two contributions made to the source $\vec{S}$, the electric field of the incident laser beam and the electric field of the Bragg reflected laser beam. Therefore $\vec{E}$ becomes the sum of both, $\vec{E} = \vec{E}_0 \cos(\omega t) + \vec{E}_{r0}\cos(\omega_r t)$. Only simple planar waves are used to keep the equations simple. Using equation 2.3 and $\vec{E}$ we get an expression for $\vec{S}$:

$$\vec{S} = -\frac{1}{2}\Delta n_0 \mu_0 \epsilon_0 n \frac{\partial^2}{\partial t^2}(\vec{E}_0(e^{it(\omega+\Omega)} + e^{-it(\omega+\Omega)} + ...) + \vec{E}_{r0}(e^{it(\omega_r-\Omega)} + ...)) \tag{2.13}$$

$$= -|\vec{k}|^2 \frac{\Delta n_0}{n}\vec{E}_{r0} \cdot \cos(\omega t) - |\vec{k}_r|^2 \frac{\Delta n_0}{n}\vec{E}_0 \cdot \cos(\omega_r t) \tag{2.14}$$

We are only looking at the incident and the Bragg reflected light, that's why the other terms of different frequencies are neglected in equation 2.13. The relations $\cos(\omega t) = \frac{1}{2}(e^{i\omega t} + e^{-i\omega t})$,

$\omega_r = \omega + \Omega$ and $\omega = |\vec{k}|c$ have also been inserted. The next step is to compare both sides of the wave equation. Because there are two frequencies, we get the following two equations, called Helmholtz equations

$$(\nabla^2 + |\vec{k}|^2)\vec{E}_0 = -\vec{S}_0 \qquad \text{and} \qquad (\nabla^2 + |\vec{k}_r|^2)\vec{E}_{r0} = -\vec{S}_{r0} \tag{2.15}$$

where

$$\vec{S}_0 = -|\vec{k}|^2 \frac{\Delta n_0}{n} \vec{E}_{r0} \qquad \vec{S}_{r0} = -|\vec{k}_r|^2 \frac{\Delta n_0}{n} \vec{E}_0. \tag{2.16}$$

These equations will help us to determine the reflectance of the first order reflected beam, here called the Bragg beam. The wavelength of light is way smaller than the wavelength of sound. For example, the laser beam for this experiment has a wavelength of 780 nm and the sound wave a wavelength of 53.3 µm. By looking at the Bragg's law ($\sin(\Theta) = \frac{\lambda}{2\Lambda}$) we can assume an incoming laser beam at a very small angle Θ. Because that angle is so small both waves, the incoming and the reflected, travel approximately in the same direction. We assume that direction of propagation is the z direction, so $\vec{E}_0 = E_0$, $\vec{E}_{r0} = E_{r0}$ and $\vec{k} \approx \vec{k}_r = k$. Furthermore we assume that the intensity of the waves are slowly varying, so E_0 and E_{r0} become, so called, envelope functions and are dependent of z. The fields E and E_r can be described as $E = E_0(z)e^{-ikz}$ and $E_r = E_{r0}(z)e^{-ikz}$.
Those two fields can now be used to solve equation 2.15, for the left side we get

$$(\nabla^2 + k^2)E = -i2k\frac{\mathrm{d}E_0(z)}{\mathrm{d}z}e^{-ikz} + \mathcal{O}\left(\frac{\mathrm{d}^2E_0(z)}{\mathrm{d}z^2}\right). \tag{2.17}$$

Since $E_0(z)$ is a slowly varying envelope the second derivative can be neglected. Comparing the right side of equation 2.17 with the right side of equation 2.15 we get

$$-i2k\frac{\mathrm{d}E_0(z)}{\mathrm{d}z} = -k^2\frac{\Delta n_0}{n}E_{r0}(z) \tag{2.18}$$
$$-i2k\frac{\mathrm{d}E_{r0}(z)}{\mathrm{d}z} = -k^2\frac{\Delta n_0}{n}E_0(z). \tag{2.19}$$

So we can write down two coupled first order differential equations

$$\frac{\mathrm{d}E_0(z)}{\mathrm{d}z} = i\frac{1}{2}\gamma E_{r0}(z) \tag{2.20}$$
$$\frac{\mathrm{d}E_{r0}(z)}{\mathrm{d}z} = i\frac{1}{2}\gamma E_0(z), \tag{2.21}$$

where $\gamma = -k\frac{\Delta n_0}{n}$.
In order to solve those equations we need boundary conditions. Let us assume that the cell expands from $z = 0$ till $z = w$ (w is the width of the medium) and that at $z = 0$ no light has

been reflected yet, that gives the condition $E_{r0}(0) = 0$. Since no light is reflected, we define a maximum amplitude at $z = 0$ for the incident laser beam $E_0(0) = E_m$. To solve equation 2.20 and 2.21 they have to be separated. Which leads to

$$\frac{\mathrm{d}^2 E_0(z)}{\mathrm{d}z^2} = -\frac{1}{4}\gamma^2 E_0(z). \tag{2.22}$$

This equation can be solved by using a harmonic ansatz and the boundary conditions. The solution is $E_0(z) = E_m \sin(\frac{\gamma z}{2}) + B\cos(\frac{\gamma z}{2})$ where B is a constant we do not know yet. With equation 2.20 we can find a solution for E_0, where B becomes zero due to the boundary conditions.

$$E_0(z) = E_m \sin\left(\frac{\gamma z}{2}\right) \tag{2.23}$$

$$E_{r0}(z) = iE_m \cos\left(\frac{\gamma z}{2}\right) \tag{2.24}$$

We have now found an expression for the rise of intensity of the reflected beam. We can therefore describe the reflectance at $z = w$ by

$$R = \frac{|E_{r0}(w)|^2}{|E_m|^2} = \sin^2\left(\frac{\gamma w}{2}\right) = \sin^2\left(\sqrt{R_w}\right), \tag{2.25}$$

where $R_w = \frac{\pi^2}{\lambda^2}(\Delta n_0)^2 w^2$ is the weak sound reflectance [1]. Equation 2.25 is the exact expression for the reflectance. It is very important to point out that R_w is proportional to the intensity of the sound wave, $R_w \propto (\Delta n_0)^2 \propto (\sqrt{I_s})^2 = I_s$ (from equation 2.5). This proportionality can be experimentally verified (figure 9)

2.2 Setup and characterization

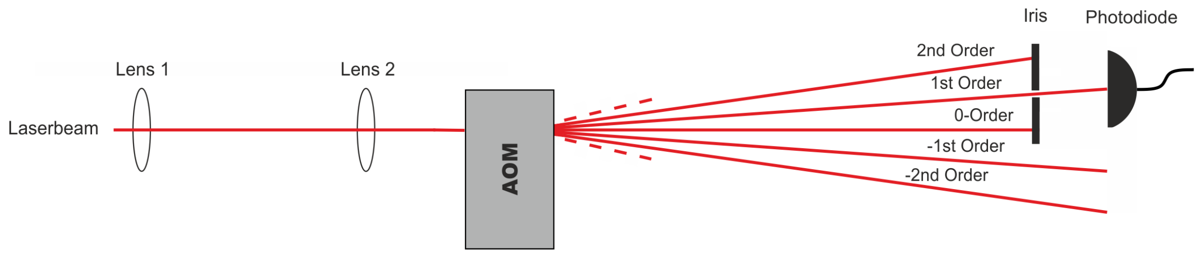

Figure 3: Setup for testing the AOM

Figure 3 shows the setup, which is used to characterize the switching speed and the efficiency of an AOM. The laser beam is a Gaussian beam (see figure 4). Lens 1 and Lens 2 are used as a telescope. Since we want the AOM to be used as a switch and a modulator, we are looking at the first order refraction. The first order or the minus first order is refracted with a lot higher efficiency than any other orders.
At first a laser beam is brought to the workspace by coupling it into an optical fiber, which runs to the setup. The next step is to measure the beam using the Matlab program Beam_Master_3. Figure 4 shows the beam profile of the laser beam coming out of the fiber. The beam radius of

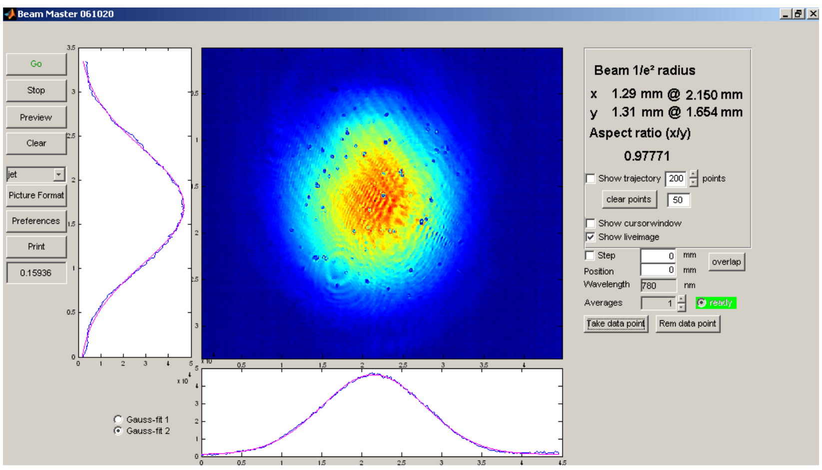

Figure 4: Beam analysis with Beam_Master_3

a Gaussian beam is defined as where the intensity of the beam profile has dropped to $\frac{1}{e^2}$ of its maximum intensity. The size of the input beam has to be known to calculate the beam waist inside the AOM. In this case the beam waist in front of the telescope is 1.30 mm. The height of the AOM crystal is 1 mm, so the beam has to be small enough to be fully inside the crystal, therefore no beam waist bigger that 500 µm is useful. Knowing the incoming beam waist and the focal length of lens 1 and lens 2, the beam waist going into the AOM can now be calculated. Table 1 shows the used lenses and the calculated beam waists.

Table 1: Calculated beam waists

Focal length of lens 1 [mm]	Focal length of lens 2 [mm]	Beam waist [µm]
200	50	325
300	50	217
200	25	170

The AOM is put close to Lens 2, so for small beam waists, the AOM stays within the Rayleigh length. The Rayleigh length is the length (in the direction of propagation) for which the laser radius stays within $\sqrt{2} \cdot w_0$ of the beam waist (w_0).
The position of the AOM has to be adjusted, so the laser beam passes the AOM centered. In the next step the iris is placed far enough from the AOM on the optic table, so that the first order can be isolated. In order to adjust the AOM correctly, a power meter is put behind the iris. The power of the first order beam is very sensitive to a correct adjustment. Therefore the AOM is put on an adjustable mount which allows a very precise adjustment. After the first order power is maximized, all necessary measurements can be done.

AOM-Driver voltage input

The amplitude of the sound wave inside the AOM can be changed by a voltage input at the AOM-driver. The amplitude of the sound wave has its maximum at 1 V and is switched off if 0 V is applied to the input. The behavior between input voltage and power that is sent to modulate the sound wave will be discussed later.
A power supply and a power meter are used to measure the power of the first and minus first order refracted laser beam in steps of 0.05 V from 0 V to 1 V. The results for each waist are shown in figure 5, 6 and 7.

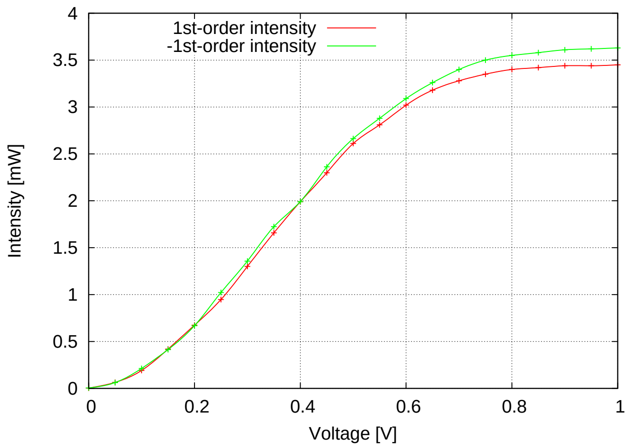

Figure 5: 1st and -1st order intensity versus the voltage input at the AOM-device for a waist of 170 µm

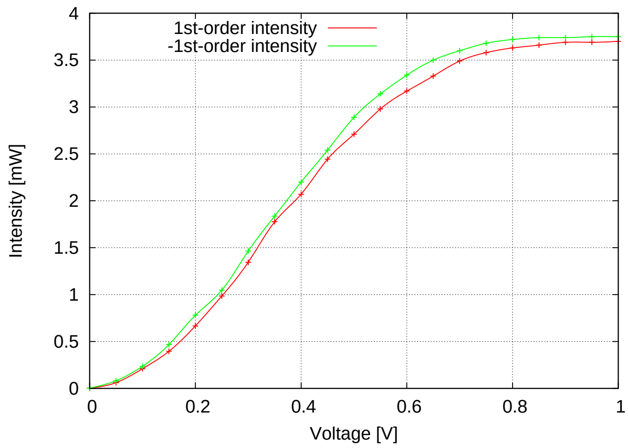

Figure 6: 1st and -1st order intensity versus the voltage input at the AOM-device for a waist of 217 µm

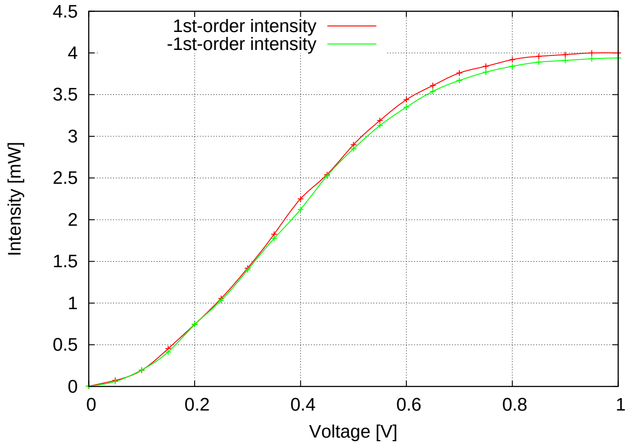

Figure 7: 1st and -1st order intensity versus the voltage input at the AOM-device for a waist of 325 µm

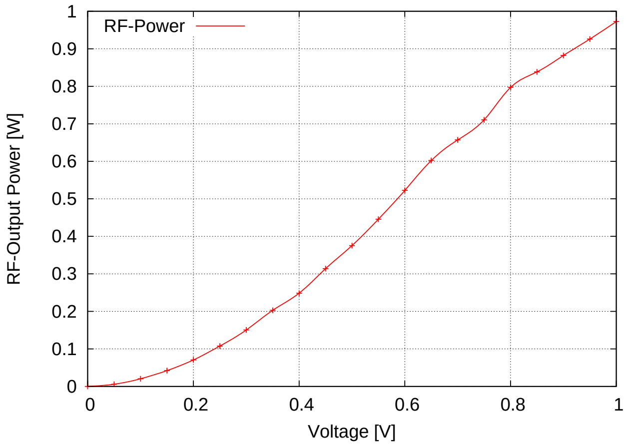

Figure 8: RF-Output power against the input voltage at the AOM-device

In figure 5, 6 and 7 we can see that the intensity for the first or minus first orders is pretty much the same. For voltages close to 1 V the power of the laser beam goes into saturation. The reason for that will be analyzed. The input voltage is connected to the power that modulates the sound wave, called the RF-Output. Figure 8 shows the RF-Output power plotted versus the input voltage. For an input voltage up to 0.6 V the RF-power is directly proportional to the intensity of the laser beam. But the RF-power increases linearly for higher voltages, while the intensity of the laser beam goes into saturation and therefore the refractance as well. Now we can compare the RF-Output power to the intensity of the first order laser beam. Figure 9 shows exactly this behavior. While the RF-Output power increases linearly, the intensity of the first order laser beam reaches its saturation. Let us now use equation 2.25 to analyze figure 9. R_w is proportional to the intensity which modulates the sound wave, meaning the RF-Output power. By using the theoretical expression to fit the data, we can verify the theoretical expression. $f(x) = (a \cdot \sin(\sqrt{b \cdot x}))^2$ is used as a fit function. The results for the parameters are: $a = 3.65$ with an uncertainty of 0.13 % and $b = 2.50$ with an uncertainty of 0.62 %

Efficiency

The next step of the AOM-characterization is to look at the efficiency with respect to the beam waist. Table 2 shows the efficiency of each beam waist. A forth beam waist is added by removing lens 2. Lens 1 is moved to a position where its focal length is the distance to the AOM, which results in a very small waist of approximately 20 µm.

Since the inaccurateness of power meter has not been considered, we will assume a mistake of 2% for the measured data. The calculated standard deviation of the efficiency is included in table 2.

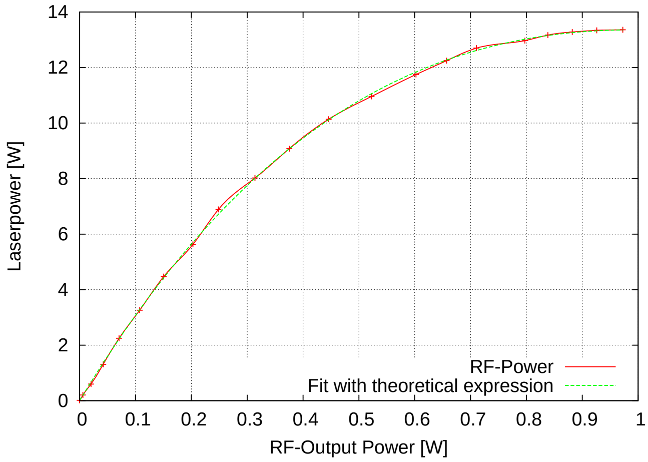

Figure 9: First order laser beam plotted against the RF-Output power

Table 2: Efficiency with respect to the beam waist

Beam waist [μm]	Order []	Input [mW]	Output [mW]	Efficiency [%]
325	1st	4.44	4.00	90.1 ± 3.6
	-1st	4.44	3.94	88.7 ± 3.6
217	1st	4.25	3.70	87.1 ± 3.5
	-1st	4.25	3.75	88.2 ± 3.5
170	1st	4.40	3.55	80.7 ± 3.2
	-1st	4.40	3.63	82.5 ± 3.3
20	1st	48.10	21.36	44.4 ± 1.8

We can see that the smallest beam waist has a rather bad efficiency, whereas the bigger waists hardly differ. Generally we can make the assumption that the bigger the waist the higher the efficiency.

Switching speed of an AOM

Another very important characteristic of an AOM is its switching time with respect to the beam waist. A function generator is used to modulate the AOM and is set to $1\,V_{pp}$ with an offset of 0.5 V. The Photodiode that is used has a bandwidth of 10 ns [7].

Beam waist of 325 μm

A 10 kHz rectangle function is applied to the AOM driver, the result is shown in figure 10. We can see that for this frequency the switching process is working very well. In the next step higher frequencies are applied to the AOM driver, 100 kHz, 1 MHz and 10 MHz. Figure 11 shows that the rectangle function is still comparable to the input function at 100 kHz. But looking at figure 12, which shows the 1 MHz modulation, it is obvious that the output signal is not a perfect rectangle function anymore. A slope from any of these measurements can be used to measure the rise time. The rise time is defined as the time that it takes the signal to rise from 10 % to 90 % of its maximum intensity. The rise time is 79 ns. The last measurement for this beam waist is at 10 MHz and shown in figure 13. Since it takes 79 ns for the signal to rise from 10 % to 90 % the signal cannot reach the height that it could reach at lower frequencies. So the rectangle function becomes a sinus like function and therefore a frequency of this order is not recommended for modulating the AOM.

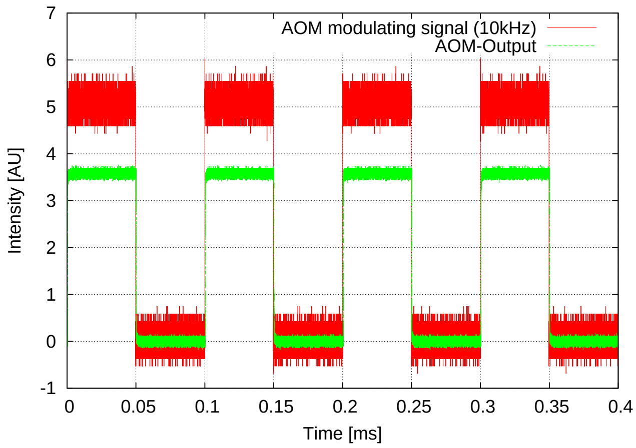

Figure 10: AOM modulating signal and output signal at 10 kHz

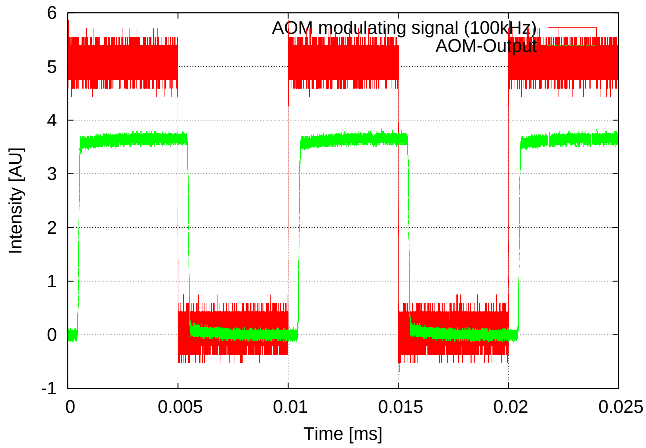

Figure 11: AOM modulating signal and output signal at 100 kHz

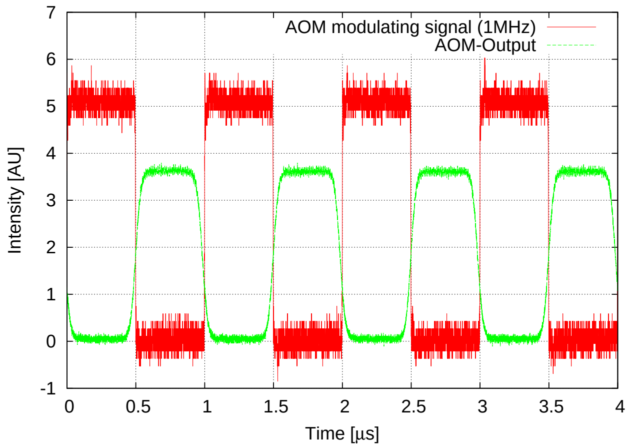

Figure 12: AOM modulating signal and output signal at 1 MHz

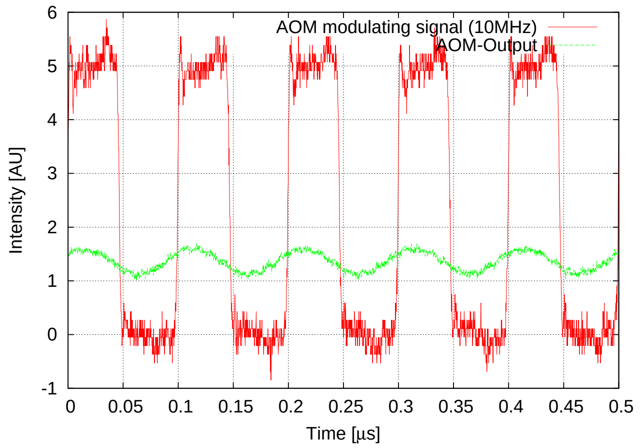

Figure 13: AOM modulating signal and output signal at 10 MHz

It might be interesting to know whether the modulation frequency affects the efficiency of the AOM. Figure 14 shows the modulation signals with different frequencies and two reference signals. The reference signals are measured by applying a constant signal at 1 V and 0 V. In order to look at the intensity, the timescale has to be rescaled. In figure 14 this consideration seems to be unnecessary, but for smaller beam waists it is not.

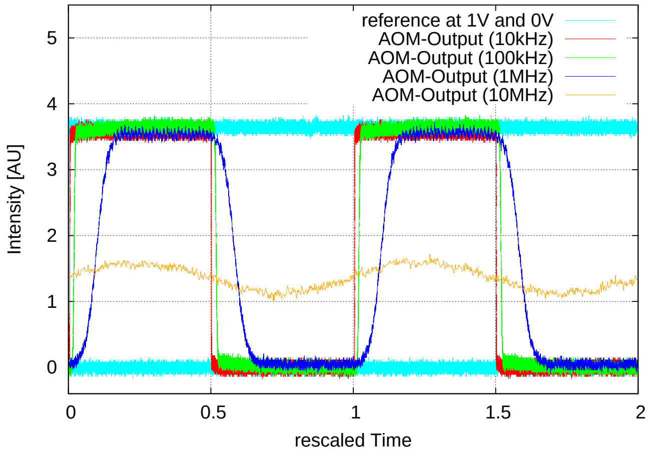

Figure 14: AOM output at different frequencies with two lines of reference

The maximum of each signal is analyzed and compared to the reference signal. The results are listed in table 3.

Table 3: Efficiency with respect to the modulating frequency

Frequency [kHz]	Intensity with respect to the reference [%]
10	~ 100
100	~ 100
1000	97
10000	14

Beam waist of 217 µm

The measurements for different beam waists are all the same. The rise time is determined for the 1 MHz modulation and is 57.6 ns. Figure 15 shows the intensity of the different frequencies and the reference signals. The results are shown in table 4.

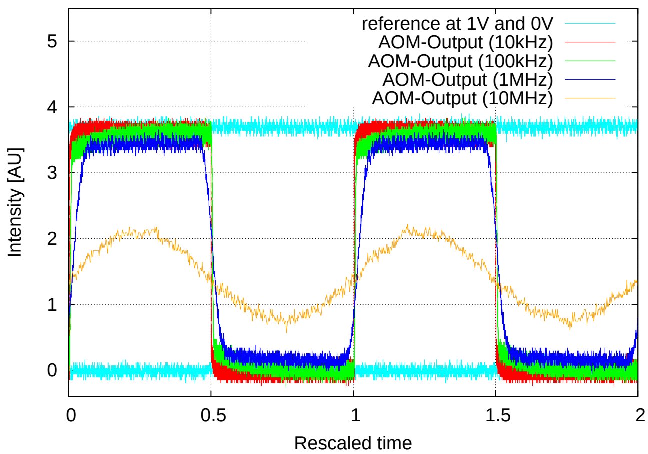

Figure 15: AOM output at different frequencies with two lines of reference

Table 4: Efficiency with respect to the modulating frequency

Frequency [kHz]	Intensity with respect to the reference [%]
10	~ 100
100	96
1000	90
10000	37

Beam waist of 170 μm

The rise time for this beam waist is 32.9 ns. Figure 16 shows the intensity of the different frequencies and the two reference signals. We can see that the rising slope ends in a peak that has not appeared for the other beam waists. The peak also appears on the modulating signal (see figure 17), so it is not caused by the AOM. It might be caused by a different function generator that is used, or a reflection in the cable, but it does not affect the measurements. The efficiency is shown in table 5.

Table 5: Efficiency with respect to the modulating frequency

Frequency [kHz]	Intensity with respect to the reference [%]
10	99
100	93
1000	87

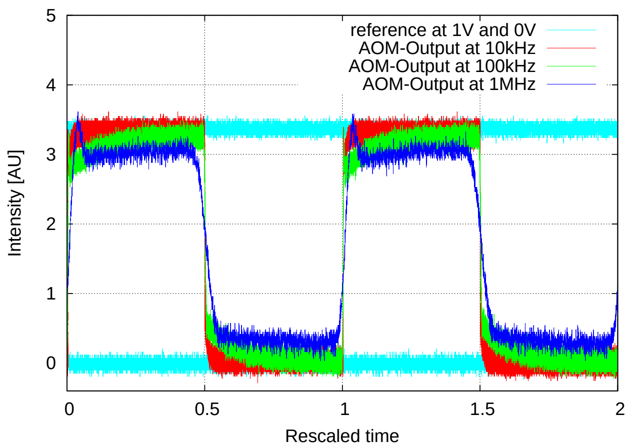

Figure 16: AOM output at different frequencies with two lines of reference

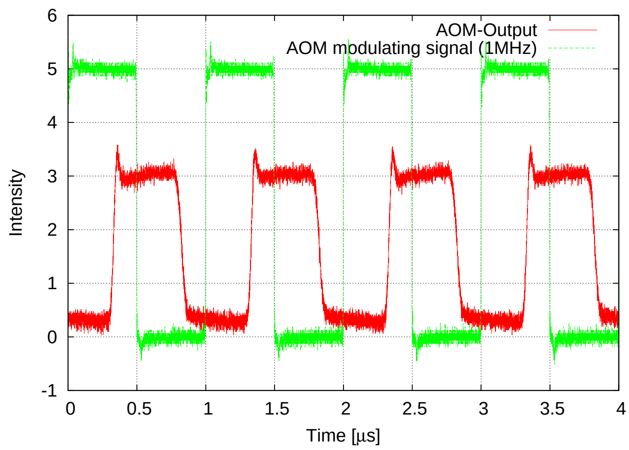

Figure 17: AOM output signal at 1 MHz

Smallest switching time

Even though we have reached a switching time of 32.9 ns we are interested in the smallest switching time that is possible. So we use the 20 μm beam waist configuration. Figure 18 shows the output signal at 10 kHz. The incoming laser beam in front of the telescope has changed (only

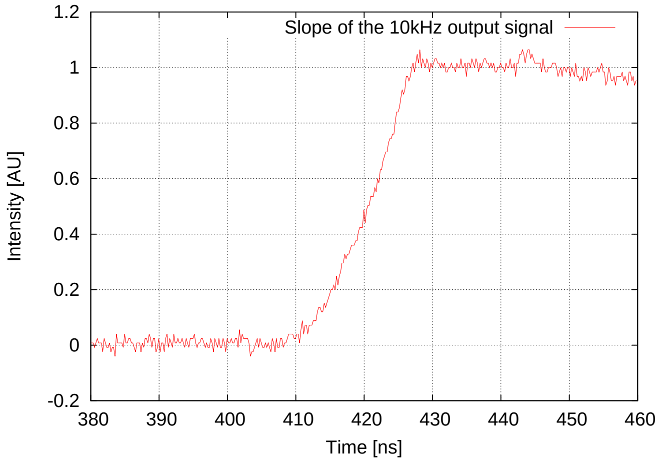

Figure 18: AOM output at 10 kHz

for the 20 µm beam waist). The laser beam is coming from a laser that another Bachelor student has built and its profile is shown in figure 19. The rise time for this small waist is 14.9 ns. The switching times are listed in table 6, we can see that the bigger the beam waist the slower the rise time. The reason for that is the transit time of the acoustic wave across the optical beam width. In order to calculate the velocity of sound, by using the measured data, we need to consider the way the rise time is measured. So the first 10 % and the last 10 % of the beam intensity with respect to the diameter can be neglected, because the rise time measurement is also taken for only 80 % of the slope. By using the intensity for a Gaussian beam $I(r,z) = I_0\left(\frac{w_0}{w(z)}\right)\exp\left(\frac{-2r}{(w(z))^2}\right)$ [1] the correct diameter that is responsible for 80 % of the intensity can be calculated. The velocity of sound can now be determined by using velocity $= \frac{\text{length}}{\text{time}}$ and averaging the velocity of all four different beam waists. The velocity of sound in the AOM is $5370\,\frac{\text{m}}{\text{s}}$. The actual velocity of sound in the AOM is $4200\,\frac{\text{m}}{\text{s}}$ [9], so the calculated velocity is in the same order of magnitude.

Table 6: Switching time with respect to the beam waist

Beam waist [µm]	Switching time [ns]
325	79.1
217	57.6
170	32.9
20	14.9

Delay

If we apply a pulse to the AOM-driver-input, we do not have an immediate response. The response appears with a certain delay. In figure 11 and 12 this delay can be seen and analyzed. The results for each beam waist are listed in table 7. The delay is caused by the velocity of sound in the AOM and the length of the cables that are used. Let us assume a cable with a length of 10 m, the speed of light in a cable can be estimated to $2 \cdot 10^8\,\frac{\text{m}}{\text{s}}$. So it takes the signal

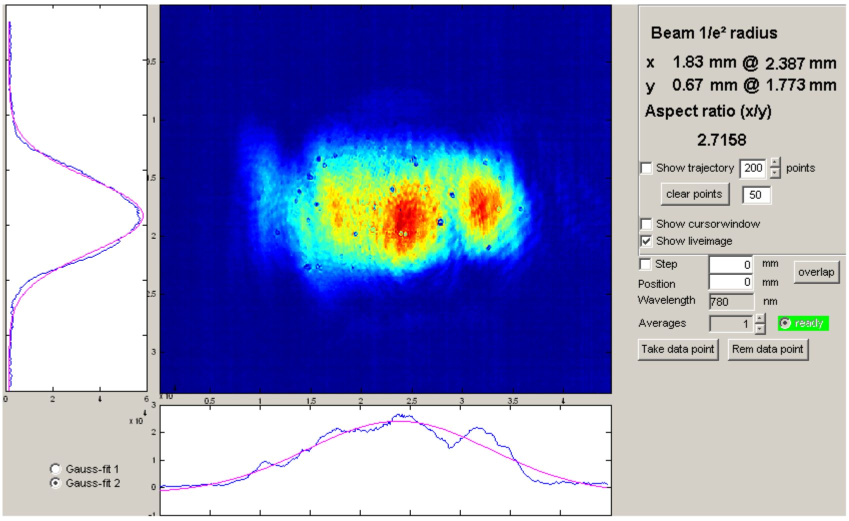

Figure 19: Laser profile of the new laser

100 ns to pass that 10 m cable. The length of the crystal in the AOM is 2.5 mm [9]. The beam passing the crystal is centered so for the propagation of the sound wave in the crystal the delay is approximately 300 ns.

Table 7: Delay with respect to the beam waist

Beam waist [µm]	Measured delay [ns]
325	480
217	350
170	320

Summary

The characterization of the AOM shows that an AOM can be used for modulating a laser beam with a switching time down to 15 ns rise time. Also, the AOM can be used as a switch without losing much laser power. For high speeds, a small beam waist is needed, which results in a bad efficiency, whereas for a big beam waist, the speed is slower but gives high efficiencies. The AOM has a minimum delay of approximately 300 ns.

3 PID-Controller

A PID-controller is an essential device for experimental physics. It can be used for many kinds of stabilizations, such as temperature, laser frequency and laser intensity. The fundamental principle of the PID-controller can be described by control theory.

3.1 Theory

Control Theory

Many systems can be represented by the model of the driven and damped harmonic oscillator, such as the control system for this Bachelor Thesis. This can be done because we want to use an external input $y(t)$ to control our system $x(t)$. The driven and damped harmonic oscillator is given by

$$\ddot{x} + \gamma\dot{x} + \omega_0^2 x = \omega_0^2 y(t), \tag{3.1}$$

where γ is the damping of the system and with k being the spring constant, $\omega_0 = \sqrt{\frac{k}{m}}$ is the resonant frequency of the system without damping. In control theory it is more convenient to analyze control systems using the frequency domain. In order to switch from time domain to frequency domain, physicists usually use the Fourier transformation. Fourier transformation is very strong especially when it comes to the symmetry between forward transformation and inverse transformation. However, in control theory it is common to use the Laplace transformation. For the Laplace transformation an exponentially decaying factor is multiplied to the function and is forcing the function to converge, so Laplace transformation can be used for a broader class of functions. In the following we will stick to the Laplace transformation, which is defined as[2]

$$\mathcal{L}[x(t)] = x(s) = \int_0^\infty x(t)e^{-st}\mathrm{d}t. \tag{3.2}$$

The frequency dependence can be determined by using $s = i\omega$. The time derivative of $x(t)$ is defined as $\mathcal{L}[\dot{x}(t)] = s \cdot \mathcal{L}[x(t)] - x(0)$ [2]. With the initial condition of $x(0) = 0$, equation 3.1 can be written as

$$\frac{\mathcal{L}[x(t)]}{\mathcal{L}[y(t)]} = \frac{x(s)}{y(s)} = \frac{\omega_0^2}{s^2 + \gamma s + \omega_0^2}. \tag{3.3}$$

We define a response function, also called transfer function $G(s) = G(i\omega) = \frac{x(i\omega)}{y(i\omega)} = \frac{\omega_0^2}{i\gamma\omega + \omega_0^2 - \omega^2}$, where $|G(i\omega)|$ is the gain and $\arg G(i\omega)$ is the phase.

A very important tool for manipulating the transfer function is the convolution theorem $G(t) * H(t) = \int_0^\infty G(\tau)H(t-\tau)\mathrm{d}\tau = G(s)H(s)$. So if the output of a system is connected to another system, their transfer functions can be convoluted in the time domain, or just multiplied

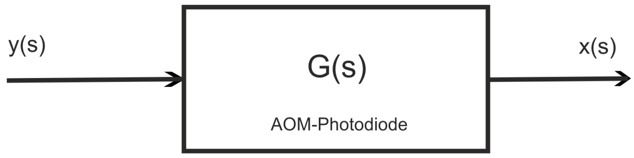

Figure 20: Response of system G(s)

in the frequency domain. The response of the System is $x(s) = G(s)y(s)$ (figure 20) or if two systems are used (where the second system has the transfer function $H(s)$) $x(s)$ can be written as $x(s) = H(s)G(s)y(s)$ (figure 21).

Let us look at a one system response again. We want the system $G(s)$ to follow a control signal

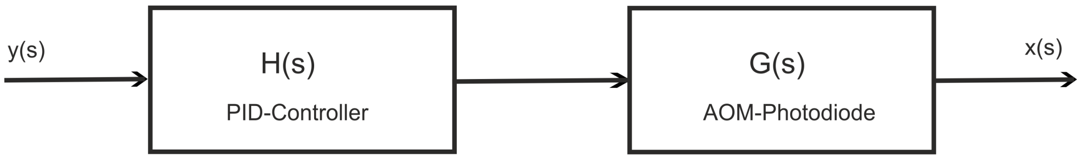

Figure 21: Response of two systems G(s) and H(s) without feedback

$r(s)$ as good as possible. We can define an error signal $\epsilon(s)$ that is the difference between the control signal and the output signal $x(s)$ that we expect $\epsilon(s) = r(s) - x(s)$. Let us now add a new system $H(s)$ right in front of $G(s)$. $H(s)$ is supposed to minimize its input, meaning the error signal. The error only gets minimized if the system is a feedback system, because without feedback, $x(s)$ cannot be subtracted from $r(s)$ and therefore $\epsilon(s) = r(s)$ for all times. So we can define the open loop (no feedback, figure 21) as:

$$x(s) = H(s)G(s)\epsilon(s) \tag{3.4}$$

And a closed loop (with feedback, figure 22) as:

$$x(s) = H(s)G(s)(r(s) - x(s)) \qquad \Rightarrow \qquad x(s) = \frac{H(s)G(s)}{1 + H(s)G(s)} \tag{3.5}$$

Where $H(s)G(s) = L(s)$ is defined as the loop gain.

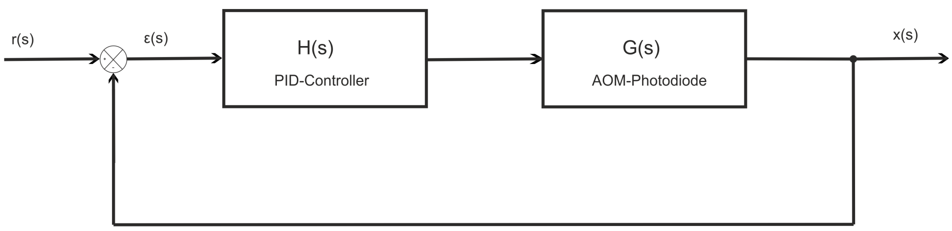

Figure 22: Feedback system

Control theory for the PID controller

The control theory discussed above is just a brief introduction for a system that can be described by a driven and damped harmonic oscillator. In this paragraph we will put the emphasis on the PID-controller. The system $H(s)$ represents the PID-controller. Where P stands for proportional, I for integral and D for derivative gain. We have to look at the error signal in the time domain. The system $G(s)$ is neglected because we are only looking at the PID-controller. So we can define the output x(t) as

$$x(t) = P\epsilon(t) + I\int_0^t \epsilon(t')\text{t'} + D\dot{\epsilon}(t). \tag{3.6}$$

P just simply amplifies the error signal. For a slow increasing of the error the emphasis of the I part increases as well, this is very good for slow controlling. Also the faster the error changes the stronger is the emphasis of the D part.
The Laplace transformation of an integral is $\mathcal{L}[\int_0^t \epsilon(t')\mathrm{d}t'] = \frac{1}{s}\epsilon(s)$ [2]. With this relation we can look at $x(t)$ in the frequency domain (by using $s = i\omega$)

$$x(i\omega) = (P - i\frac{I}{\omega} + iD\omega)\epsilon(i\omega), \tag{3.7}$$

where $x(i\omega) = H(i\omega)\epsilon(i\omega)$ and therefore the PID controller can be written as $H(i\omega) = (P - i\frac{I}{\omega} + iD\omega)$.
We can see that the different parts of the PID controller play different rolls with respect to the frequencies. I is proportional to $\frac{1}{\omega}$ and therefore responsible for low frequencies. If we look at the D-part, we will see that the higher the frequency the stronger it is. The P-part is just a constant and is good for frequencies where the I- and the D-part are low. Equation 3.7 is for open loops. When the PID controller that is used in this experiment will be analyzed, we will look at the closed loop and the attenuation.

3.2 Setup and characterization

Basic setup and output configurations

The PID-board design by Stephan Jennewein is used as a sample. At first the PID-board is soldered and built after the sample. Figure 23 is a simplified exposure of the sample. In following the operational amplifiers will be named OpAmp. The original PID-board is configured for standard lab voltages, meaning input and output voltages are in a range of −10 V to 10 V. The AOM-Device requires an input level of 0 V to 1 V. Therefore the output from the PID-controller has to be adjusted, since it is directly connected to the AOM-device input. That is the first configuration on the PID-board. Let us look at the output OpAmp. This OpAmp is chosen because we can keep the whole voltage range of the important controller parts like the P-,D-

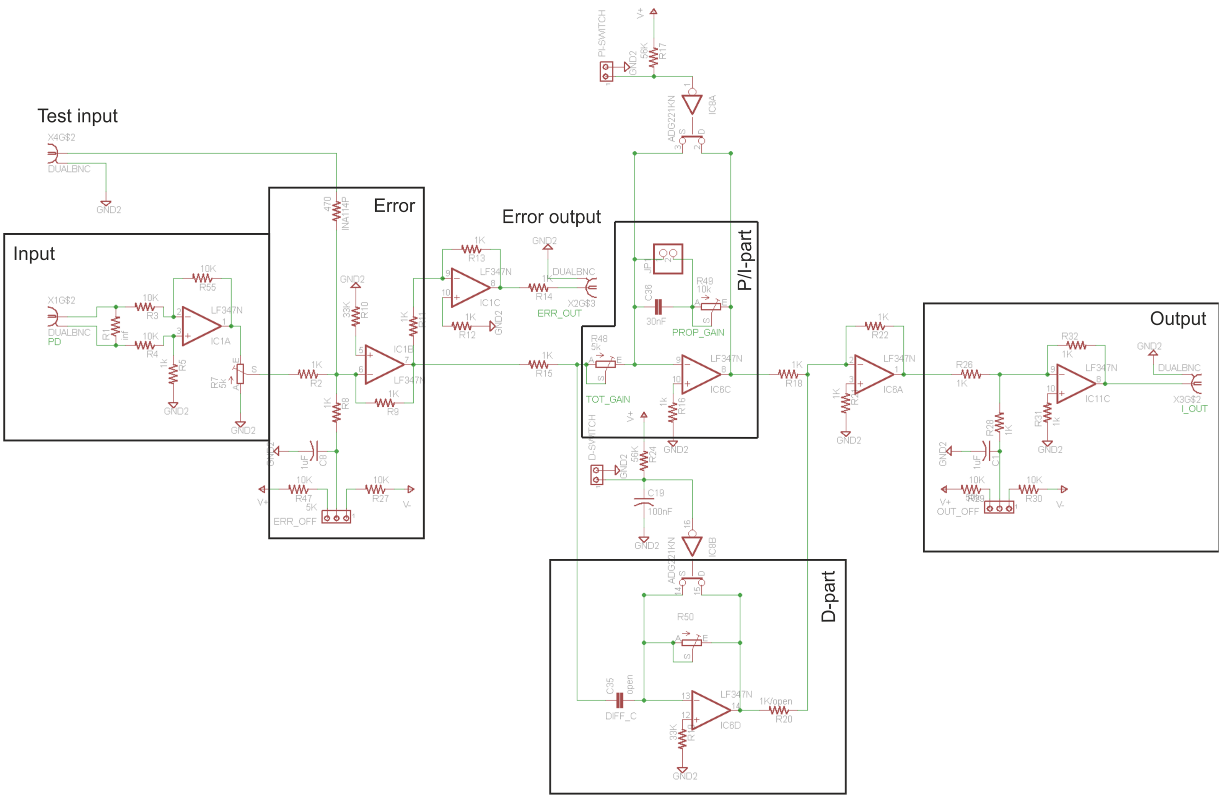

Figure 23: Simplified schematic of the PID-controller designed by Stephan Jennewein

and I-parts. As stated above the initial amplitude is 20 V_{pp}, so the gain has to be decreased. This can be done by using the standard equation for a summing circuit [8] and changing R26 to 12 kΩ and R28 to 100 Ω. Since the signal is still oscillating around the zero level, the offset has to be adjusted too. So R30 is set to 470 Ω so the offset is shifted to more positive values. Also R28 has changed the weight of the offset in the output OpAmp circuit.

Configuration of the input signal

The input signal comes directly from the photodiode. Usually a 50 Ω load resistance should be used for an outgoing signal to have a high bandwidth. For the PID-configuration R3 is responsible for the impedance, which is 10 kΩ. If impedance that high is used, the photodiode would be too slow for our system. If a 50 Ω impedance is used, we would have almost no signal. The setup is shown in figure 26, we try to keep the signal, which we want to use for stabilizing the system, as small as possible. The more signal we use to stabilize the system the lower the efficiency. That means we have to find a different solution. The signal from the photodiode at $\lambda = 780\,\mathrm{nm}$ is converted with $0.487\frac{\mathrm{A}}{\mathrm{W}}$[7]. We want to use a maximum of 1 mW laser power for stabilizing the system. That means a current of 487 µA is coming from the photodiode. Furthermore we make a measurement for the rise time of the photodiode with respect to the impedance. With an Impedance of 680 Ω the rise time is approximately 1 µs. Since we want to make sure that photodiode is fast enough we change R3 to 470 Ω. By using the input voltage U, the impedance R3 and the current I, we get an input voltage of U = R3 · I = 470 Ω · 487 µA ≈ 290 mV. Figure 24 shows a Bode plot of the control system with different impedances. We can see that the chosen configuration with 470 Ω does hardly differ from the one with 50 Ω, but the configuration with 1 MΩ is much slower.

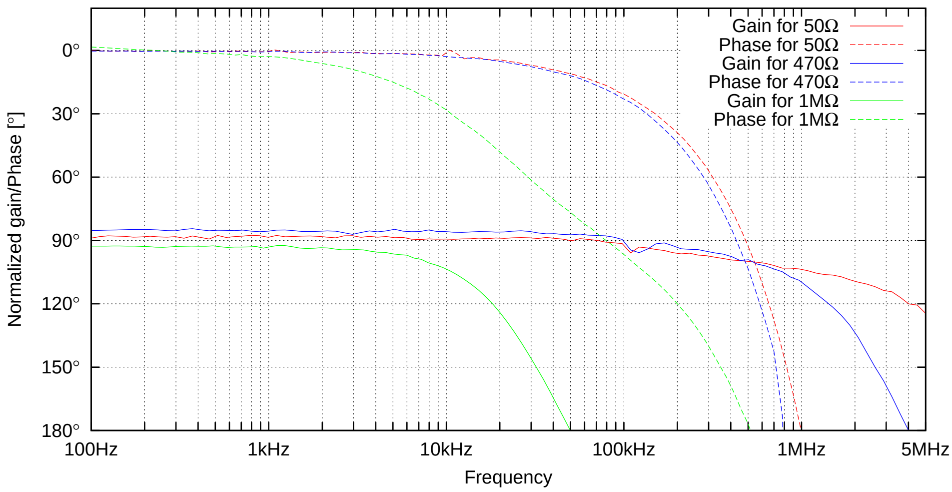

Figure 24: Frequency response of the AOM-Photodiode system with different impedances

Amplification of the input signal

Since R3 is 470 Ω the amplification of the input OpAmp circuit increased a lot. Using the equation for an amplifying circuit [8] the gain is −21.28. Using the maximum input signal the output of the first OpAmp system is $-21.28 \cdot 290\,\text{mV} = 6.17\,\text{V}$. So we can almost reach the complete voltage range of the controller.

Error signal configurations

The error OpAmp works as a summing circuit, depending on three inputs. Input one is from the input OpAmp, input two from the error offset potentiometer and input three from the "Test" input. The "Test" input or the error offset potentiometer can be used to create a reference signal we want the control system to follow. Usually we want to use either the "Test" input or the error offset not both at a time. Input one is inverse to input two and three, which means that input one is subtracted from input two or three. If the laser intensity is just as we want it we adjust the "Test" signal or the error offset so that input two or three minus input one equals zero. We have to look at the error offset, because we want to use as much range as possible from the potentiometer, therefore we need to change the emphasis of the signal in the summing circuit. So we change R8, R47 and R27 to 470 Ω. Secondly, we want the "Test" input to be used from approximately 0 V to 10 V. In figure 23 there is the INA114P OpAmp between the "Test"

input and the summing circuit. This part is not soldered so we connect a 4.7 kΩ resistor from position two to position six of that slot.
Those are the main configurations that are made. There will be some more changes but they will have to do with the complete control circuit. The PID controller can now be characterized by analyzing Bode plots.

Characterization

We analyze the bandwidth of the PID controller by using a Bode plot, which is shown in figure 25. A Bode plot is measured by applying different frequencies to a system and looking at the gain and the phase of the response, this will be done for all following Bode plots. We will now take the full control circuit into consideration. Let us assume the intensity of the signal coming into the AOM is somehow modulated with a sinus at a high frequency. The PID controller tries to keep the laser intensity constant after the AOM. Therefore an inverse (to the modulation on the laser) signal is modulated on the PID output. We can see that for high frequencies the phase starts to shift, that means the output signal of the PID has a delay. If the delay is too big the modulation on the intensity cannot be compensated anymore and even is amplified. The point of maximum bandwidth is, where the phase has shifted 45 degree [3]. We can say that that the PID-controller can be used up to a frequency of 900 kHz. Even though we have determined the switching time of the AOM, we still have to determine the bandwidth of the AOM-photodiode system. By using figure 24 the bandwidth can be determined to 200 kHz. That is rather surprising, since the switching time of the AOM is really fast. The reason for that is the delay time of all components.

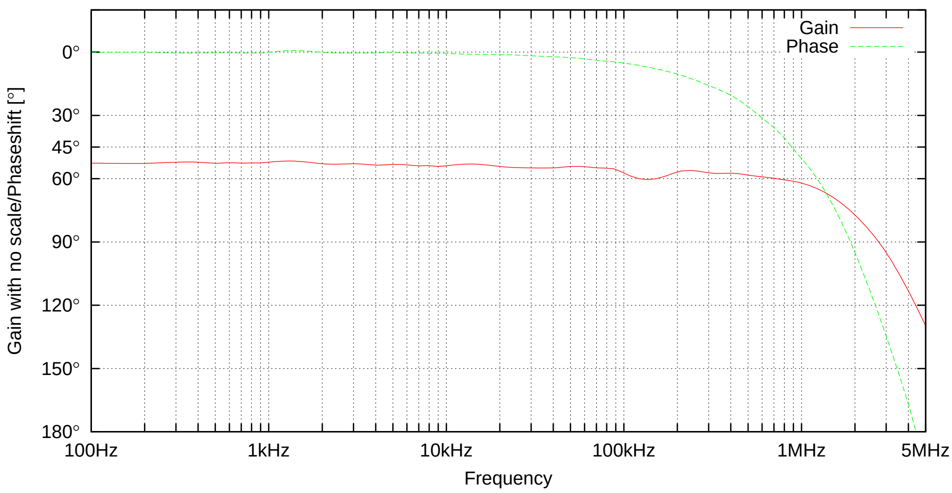

Figure 25: Bode plot of the open loop PID circuit

3.2.1 Configurations with the complete control circuit

Setup

Figure 26 shows the setup of the complete control circuit. The AOM is set up like in figure 3,

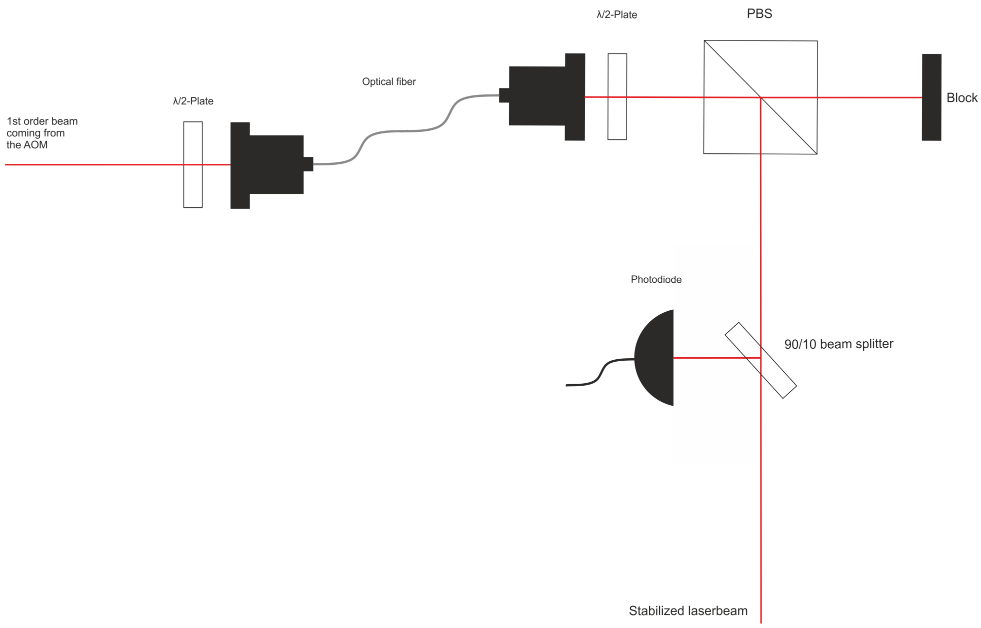

Figure 26: Setup for stabilizing the laser intensity

but instead of a Photodiode, the first order laser beam is coupled into an optical fiber. In order to maximize the intensity of the vertically polarized beam later, two $\lambda/2$-plates are put before and after the optical fiber. The PBS splits the laser beam into a beam with horizontal and a beam with vertical polarization. We use the $\lambda/2$-plates that are put before and after the optical fiber to change the polarization of the beam, so that the intensity of the vertically polarized beam is maximized. The vertically polarized beam passes a $90/10$-Beam splitter. The 90 % beam is the stabilized beam, whereas the 10 % beam is used to stabilize the system.

Configuration of the I-part

Since we have now been looking at basic configurations and the bandwidth of the PID-Controller, we need to configure the property of the control values, such as the I-part and the D-part. In figure 27 we use a Bode plot to characterize the emphasis of the I-part. In the first measurement the PID-controller is switched of. By looking at the input and the error signal output we get a reference signal. We can use it as a reference signal because the control circuit is not closed and therefore the error signal does not have any attenuation. Now the PID-controller is switched on. If we look at P/I-part OpAmp, which is an integrating and amplifying circuit, we can see that the I-part and the P-part are not independent. So R48 is responsible for the gain of the I- and the P-part, whereas R49 changes the emphasis of the I- and the P-part. So if R49 is turned to $0\,\Omega$, the P-part is switched off. If R49 is turned to its maximum, the I-part will not play a big role anymore, but we have to consider that the I-part is not completely switched off. In order to switch off the I-part we can set jumper 1. Figure 27 shows different configurations of the I- and

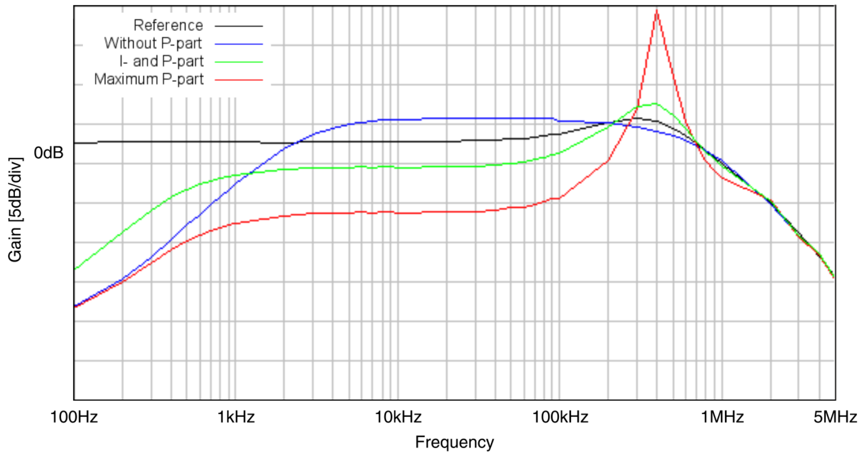

Figure 27: Bode plot for different configurations of the I-part and the P-part

the P-part. The black curve is the reference signal. If only the I-part is on we get the blue curve, if we turn up the P-part we get the green curve and if we turn it to its maximum we get the red curve. Let us analyze figure 27. The I-part is obviously responsible for the slope on the left side. Whereas the P-part is responsible for all frequencies. At around 500 kHz we can see a peak that increases for a strong P-part. That peak is the eigenfrequency of the system. If the peak is too high the system will not attenuate anymore and starts to oscillate. The eigenfrequency is caused by the delay of the system. The PID controller does not see the current signal but the signal that needed the delay time to reach the PID controller, therefore any frequencies that close to the eigenfrequency get amplified.
The configuration of figure 27 is not satisfying, since the attenuation is pretty low. In order to achieve a higher damping the frequency of the integral part is increased by replacing C36 with a faster 470 nF capacitor. Looking at figure 28 the attenuation for frequencies that are lower than 20 kHz is 20 dB with respect to the reference signal. If we look at higher frequencies we still have a pretty good attenuation, until we get close to the eigenfrequency. The maximum bandwidth for this setup is 200 kHz by looking at the phase.

Configuration of the D-part

No matter how, a configuration of the D-part did not work. Then we figured out that the D-part configuration of figure 23 is incorrect. So every time the D-part was switched on it worked as a low pass filter. In order to get the D-part working the circuit has to be modified. So we connect a 470 Ω resistor after the error OpAmp and before R15 to the circuit. The D-part can now be connected to the new resistor. The new D-part is shown in figure 29. The D-part does not affect the final setup of the control parameters a lot. In figure 28 a small D-part was already included.

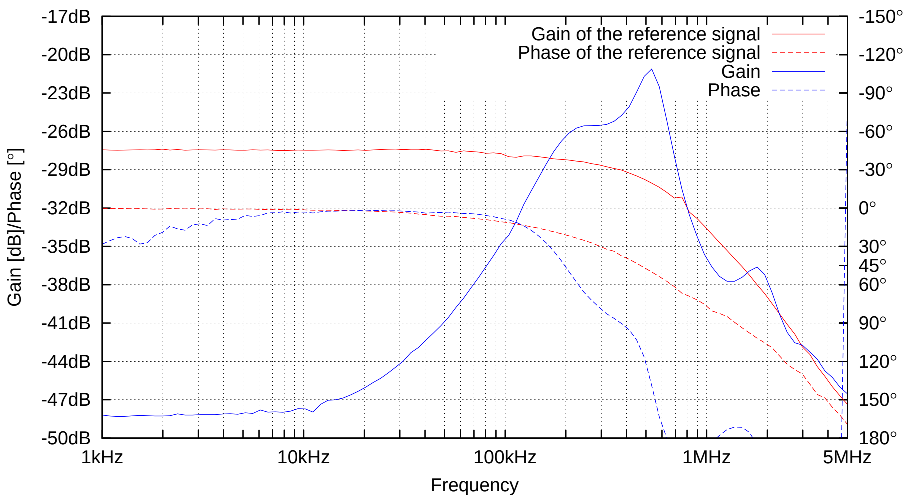

Figure 28: Final configuration of the PID-controller

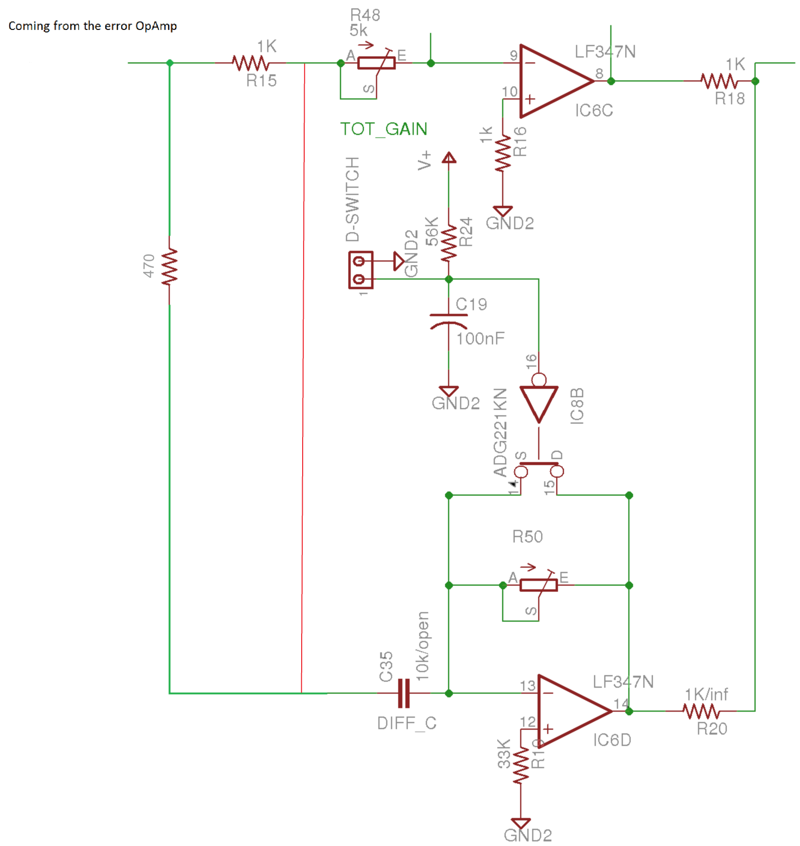

Figure 29: Fixed D-part. The red line is the old configuration

3.3 Diode system for protection

The AOM-device-input is only to be used between 0 V and 1 V. For voltages that are too high or too low this expensive device would be broken. Even though we have already configured the output of the PID controller, we want to make sure that the signal stays within a certain range.

Therefore we build a protection circuit that will be put between the PID output and the AOM-driver input. Figure 30 shows the schematic of this protection circuit. The first diode cuts off

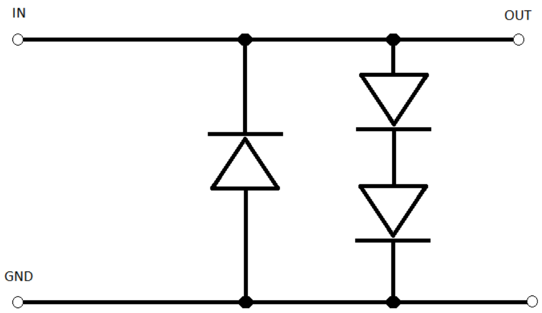

Figure 30: Diode protection configuration

the signal at $-300\,\mathrm{mV}$ and the second and third, which are connected in series cut off the signal at around $1.6\,\mathrm{V}$. Using that range we make sure that the AOM-device will not be damaged, but are not too narrow to somehow affect the control signal in its regular range. Of course we do not want the diode system to reduce the control bandwidth, so we use Schottky-Diodes that are fast enough. Figure 31 shows the Bode plot for the diode system. We can see that it is fast enough. The gain is not changed even for fast frequencies, also the phase is not shifted.

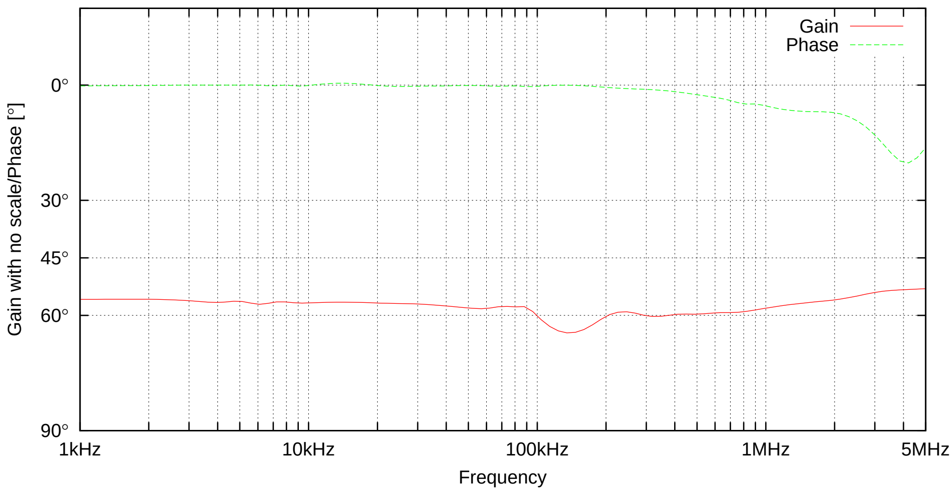

Figure 31: Bode plot for the diode system

4 Stability of the laser intensity

In order to characterize the complete setup, we have to somehow find a way to directly see the controlling. We need to change the setup, so we replace the laser blocker from figure 26 with a second photodiode. The first photodiode is measuring the vertically polarized laser beam and the second photodiode the horizontally polarized laser beam. The idea is to stabilize the system, but only for one polarization. The other polarization will still change its intensity, so we can watch the control circuit work.

Figure 32 shows a 30 min intensity measurement of the free running system for both polarizations. We want to verify that the system keeps the stability of the laser intensity constant, even if the optical fiber is mechanically influenced. Those influences were done to the fiber at around 50 s and at around 1250 s and cause a change of intensity for more than 1 mW.

Figure 33 shows the 30 min measurement for the stabilized laser system. The laser intensity has to be reduced, because for the free running measurement, we used the AOM at its maximum output power. By looking at the horizontally polarized light beam, we can see that at around 200 s some influence on the optical fiber happened, but the laser intensity for the stabilized vertically polarized light remains stable.

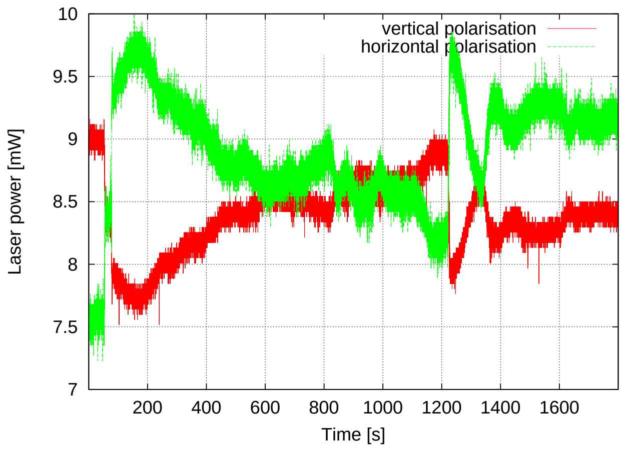

Figure 32: 30 min measurement for the free running system for both polarizations

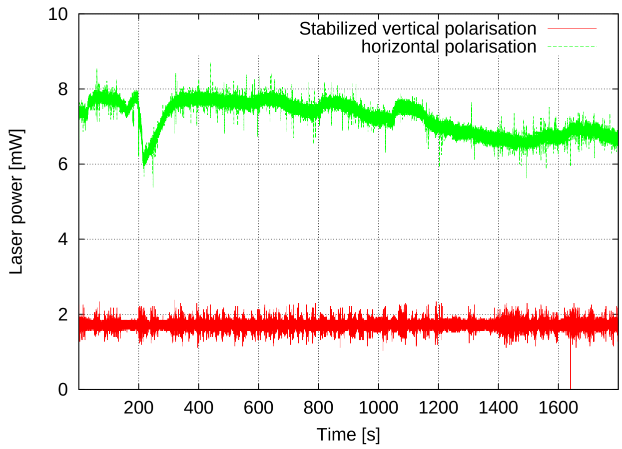

Figure 33: 30 min measurement for the stabilized system for both polarizations

The intensity of the laser beam is full of noise. Unfortunately the noise is a high frequency noise that cannot be compensated by the PID-controller. The PID-controller is only partly responsible for the noise, most of the noise is also there even without attaching the PID-controller. If we compare the free running system with the stabilized system, we can see that the fast noise seems to be the same on both measurements.

Sample variance The sample variance can be used to measure the stability of a time dependent signal such as the laser intensity $I(t)$. It can be expressed as [5]

$$\sigma_I^2(N) = \frac{1}{N-1}\sum_{i=1}^{N}\left(\Delta I_i - \frac{1}{N}\sum_{j=1}^{N}\Delta I_j\right)^2 , \tag{4.1}$$

where N is the number of samples. N is connected to the time between two samples τ and the length of the interval T by $T = \tau \cdot N$. With equation 4.1 the sample standard deviation can be expressed by the square root of the sample variance. Figure 34 shows the sample standard deviation for the free running and the stabilized system. The time between two samples is

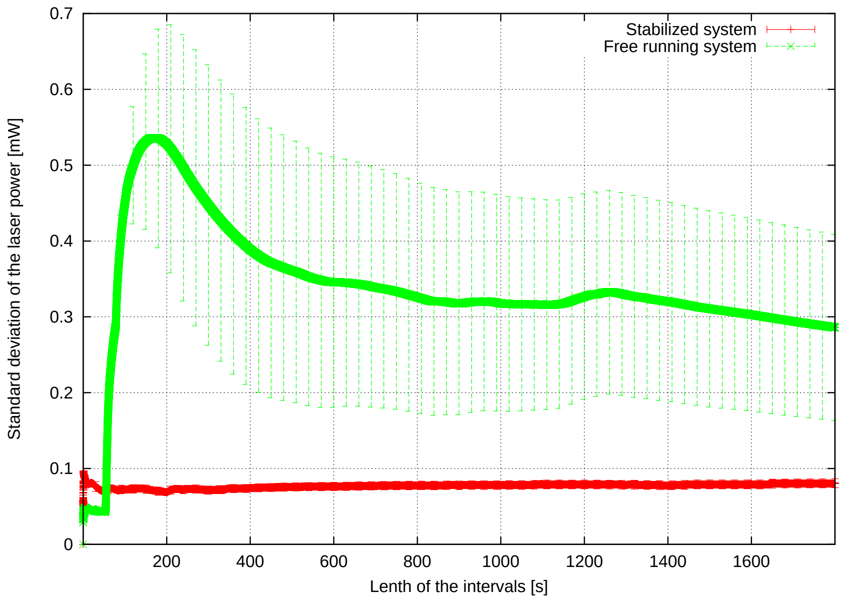

Figure 34: Sample standard deviation for the free running and the stabilized laser

10 µs, this is caused by the resolution of the oscilloscope for long term measurements. Figure 34 can show the stability of the system. So we can see that the standard deviation of the laser is approximately 80 µW for long timescales. If we look at short times, the fast noise becomes more important and the stability of the system is getting worse. In order to understand the small intervals let us look at figure 32 again, for the first thirty to fifty seconds the free running vertically polarized laser beam is almost stable. If we compare this to figure 34 than we can see that, indeed, the first small intervals seem to be stable. But we can also see that the noise of the free running system is about 50 µW, whereas the rest of the noise of the stabilized laser beam is mainly caused by the eigenfrequency amplification of the PID controller.

5 Summary and outlook

This thesis was about stabilizing the intensity and polarization of a laser. The stabilizing system consists of an acoustooptical modulator, a PID-controller and a few additional components. Every component was analyzed, at first the AOM.
The efficiency of an AOM is dependent on the beam waist of the laser beam, but the beam waist also affects the switching time of an AOM. For a big beam waist we could reach an efficiency of 90 %. For a very small beam waist we even could achieve a rise time of 15 ns. The bandwidth of the AOM photodiode system is 200 kHz due to the delay time of the AOM and any other transfer length.
In this bachelor thesis, a PID-controller was built and customized for the AOM-system. The PID-controller could achieve a bandwidth of 900 kHz.
The complete control circuit can be used up to a bandwidth of 200 kHz with an attenuation of 20 dB for a bandwidth up to 20 kHz. The intensity stabilization is meant to be a long term stabilization, its stability is 80 μW for the system that was built during this bachelor thesis. It can be very useful for compensating the drift of the laser intensity, for example, after an optical fiber.

Outlook

An input can be used to stabilize the laser intensity to a certain height. But for some cases we want to pulse the laser intensity, by using the "Test" input. So the question that will be dealt with in the future is, if the intensity of the pulse is stabilized well enough and how fast can the pulsing be. Another future project is to see if we can use very fast pulses that do not get recognized from the PID-controller. This could be possible because the AOM has a rise time that is faster than the capability of the system to response.

References

[1] Bahaa E. A. Saleh, Malvin Carl Teich: *Fundamentals of Photonics*, Wiley (1991)

[2] W. Kimmerle: *Mehrdimensionale Analysis und Differentialgleichungen*, edition EAE delkhofen (2010)

[3] J. Bechhoefer: *Feedback for physicists: A tutorial essay on control*, Rev. Mod. Phys. Vol. 77, 2005

[4] M. Zwierlein: *A short introduction to Feedback Control*, 2008

[5] Jonathan Balewski: *Hochauflösende Photoassoziationsspektroskopie von Rydberg-Dimeren und Trimeren*, Diplomarbeit, 2009

[6] Robert G. Hunsperger: *Integrated Optics, Theory and Technology, Fourth Edition*, Springer (1995)

[7] http://www.thorlabs.com/Thorcat/13000/DET10A-SpecSheet.pdf (13. Aug 2012, 14:22)

[8] H.J. Bauer, S. Döttinger, A. Grupp: *Physikalisches Praktikum, Elektronik*, Physikalisches Institut der Universität Stuttgart (2009)

[9] http://www.crystaltechnology.com/docs/97-01280-.pdf (15. Aug 2012, 16:46)

6 Acknowledgment

I want to thank everybody for supporting me. A special thanks to

- Prof. Dr. Tilman Pfau, who made this thesis happen
- Dr. Sebastian Hofferberth, who was my supervisor and was there if any help was needed.
- Michael Schalgmüller, Stephan Jennewein, Christoph Tesp and Huan Nguyen, who supported me where ever I needed help or advice.
- Wolfgang Voesch and Udo Hermann